Circuital Modeling of a Droplet Electrical Generator

Luigi Costanzo, Alessandro Lo Schiavo, *Senior Member, IEEE*, and Massimo Vitelli

***Abstract*—A droplet electrical generator (DG) is an energy harvester able to scavenge energy from water droplets sliding on its surface. A compact electrical model of a droplet generator is here presented together with a black-box identification procedure. Even if previous research works have shown the great potential of the droplet generator in terms of extracted power and have investigated the optimization of the device, a simple equivalent electrical circuit is not available, which is fundamental for predicting its behavior and for designing its electronic interface, devoted to maximizing the power extraction under varying source and load conditions. A detailed identification procedure for the model parameters is also presented, in order to overcome the issues due to the high voltage, low current, high bandwidth, and unknown time-waveform of the time-varying capacitances. It is also shown how the proposed model allows the designer to predict analytically and numerically the energy that can be extracted by the generator. Finally, experimental tests are presented to show that the proposed model and the outlined procedure are able to effectively predict with good accuracy the system behavior under different operating conditions.**

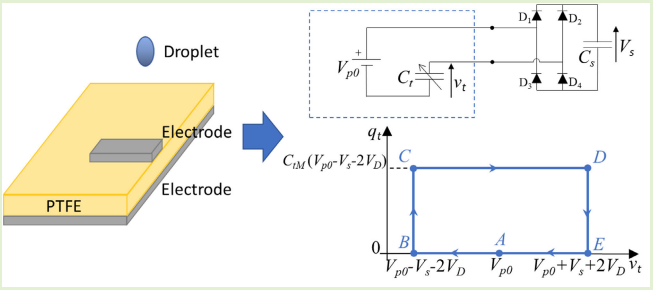

***Index Terms*— Circuit analysis, circuit modeling, energy harvesting, parameter identification.**

I. Introduction

THE eco-friendly solution for supplying devices in wireless sensor networks is represented by energy harvesters that are able to locally convert into electricity otherwise wasted forms of energy available in the surrounding environment [1], [2]. Even if many sources of energy can be exploited, like sun, wind, vibrations, electromagnetic fields, and so on, the most ubiquitous one is water. For this reason, many research efforts have been recently devoted to scavenging energy from raindrops [3]. The traditional method consists in collecting raindrops into reservoirs and in generating electricity through microturbines and electromagnetic generators. However, turbines are inefficient with low water supply and generators are bulky and heavy. Energy harvesters exploiting the kinetic energy of free-falling droplets impacting on piezoelectric cantilevers were investigated in [4] and [5], but very low energy levels, around 1 nJ per droplet [4], can be extracted mainly due to the resonant nature of piezoelectric cantilevers.

Manuscript received 5 April 2023; accepted 15 April 2023. Date of publication 27 April 2023; date of current version 14 June 2023. This work was supported in part by Università degli Studi della Campania Luigi Vanvitelli in the framework of "Piano Strategico di Ateneo 2021-2023—Azione strategica R1.S2" under Grant SCAVENGE. The associate editor coordinating the review of this article and approving it for publication was Dr. Yongjia Li. *(Corresponding author: Alessandro Lo Schiavo.)*

The authors are with the Department of Engineering, Università degli Studi della Campania "Luigi Vanvitelli," Aversa, 81031 Caserta, Italy (e-mail: luigi.costanzo@unicampania.it; alessandro.loschiavo@unicampania.it; massimo.vitelli@unicampania.it).

Digital Object Identifier 10.1109/JSEN.2023.3269565

To overcome the above drawbacks, several water energy-harvesting techniques that rely on the generation and transfer of interfacial charges have been developed in the last years [6], [7]. Reverse electrowetting energy harvesting, exploiting the mechanical variation of the electrical double layer (EDL) capacitance of a droplet squeezed between two electrodes by an external mechanical source, has emerged as an efficient technology able to generate power at low modulation frequencies [8], [9]. The electrostatic harvesters developed in [10] and [11] are also based on the capacitance variation induced by a conductive droplet freely sliding on an electret film sputtered onto interdigital electrodes.

As an alternative to exploiting variable capacitances, water droplets can be used for generating triboelectricity through the contact electrification between the water and a triboelectric insulating polymer film. The conjunction of contact electrification and electrostatic induction in a single electrode harvesting device led to a promising droplet-based triboelectric nanogenerator (TENG) [12], featuring a simple structure, low-cost material fabrication, and good low-frequency characteristics. The desire for a superhydrophobic insulating surface, which ensures timely refresh of contact sites from droplets, and the drawback of a superhydrophobic surface, which reduces the effective contact area of impinging droplets, led to the development of a porous surface for TENG devices [13], exhibiting higher power together with optical transparency, useful for hybrid generation from raindrop and sunlight [14].

A significant increase in the power generated by a TENG was reached by the so-called droplet electrical generator

(DG) [15], through the addition of a second electrode over the insulating film, to obtain a closed-loop electrical system. Further significant improvements in the generated power have been made possible by optimizing the effects of electrode geometry and droplet parameters (volume, conductivity, and dropping frequency) [16] and by tailoring parameters, such as dielectric layer thickness, droplet ion concentration, and external load [17]. These improvements have resulted in a harvested energy per droplet of 650 nJ, with an average power density per pulse of 357 W/m^2 in [17].

Even if the above DG devices represent a real turning point in the development of raindrop-based energy harvesters, an efficient electrical model that can be employed for designing the optimal electronic interface for these devices is still missing. Indeed, the electrical power that can be extracted by energy harvesters is a function not only of the energy source and the harvesting device, but it strongly depends also on the harvester's electrical load [18], [19], [20]. First attempts to develop electrical models of DGs based on their physical behavior were proposed in [15], [16], and [17], but they are not simple enough for design purposes. An interesting numerical analysis was developed in [21], but it is only focused on the spreading process of a droplet impacting the insulating surface.

To overcome the above gaps, in this article, a compact electrical model of a DG device is developed by showing that it can be reduced to a triboelectric-based electret nanogenerator [22], made up of a dielectric layers with injected charges, which separates two conductive electrodes moving with respect to each other. The resulting model makes it easier to understand, visualize, and simulate the DG device behavior in different operating conditions and allows checking the performance of different electronic circuits without the need of making a physical DG [23]. Thus, the model can be usefully exploited for the analysis and the design of energy harvesters based on DGs.

Moreover, a simple approach to the identification of the parameters of the equivalent electric circuit of the DG is shown, overcoming the limitations of the typical identification approaches [22]. Differently from typical triboelectric-based electret nanogenerators, the considered DG is characterized by open circuit voltages up to hundreds of volts and currents that can be as small as a fraction of nanoamperes. Besides, typical DG voltage waveforms can exhibit rates of voltage increase as high as hundreds of volts per microsecond. These characteristics require very demanding measuring electronic interfaces or, as an alternative, they impose to take into account the effect of the measuring interface on the device under test. Moreover, usual procedures for parameter identification assume that the trend over time of the variable capacitance is known, while in the considered case such a trend depends on how the contact between the droplet and the electrode evolves in time, and it is unknown. In this article, an identification procedure is presented, which takes into account the ohmic-capacitive impedance of the probe and is able to estimate the time waveform of the variable capacitance.

Finally, by exploiting the presented model, an analytical expression of the energy extracted by the DG is deduced as a function of the characteristics of the droplet generator and of the bridge rectifier. The relationship, which provides valuable insight into the harvesting mechanism, can be usefully exploited by the system designers.

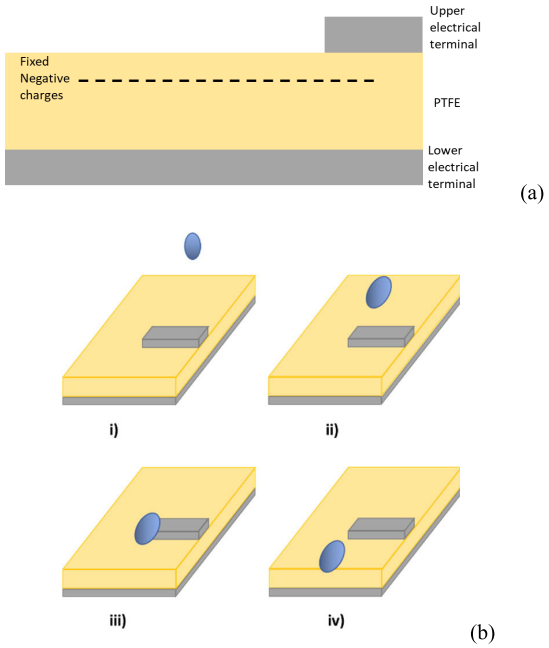

Fig. 1. (a) Schematic of a DG. (b) Operation over time of a droplet generator. i) Droplet falling; ii) droplet flowing on the surface; iii) droplet contacting the upper electrode; and iv) droplet leaving the upper electrode.

The rest of the article is organized as follows. In Section II, the equivalent circuit of a DG is presented. In Section III, an identification procedure is outlined, whereas in Section IV, an analytical estimation of the energy extracted for each droplet is proposed. Finally, simulations and experiments are presented in Section V.

II. Equivalent Circuit of a DG

A DG is made up of a solid dielectric layer with trapped charges near the upper surface, a lower conductive layer acting as the lower electrode, and finally, a conductive terminal placed above the dielectric acting as the upper electrode, as shown in Fig. 1(a) [15]. A typical material employed for the dielectric layer is represented by the PTFE (PolyTetraFluoroEthylene, also called Teflon), an electret material with high charge storage capability and stability. The negative charges prestored in the dielectric surface are formed through continuous droplet impingement or precharging on its initial neutral state, in order to obtain a saturated surface charge density, which is essential for high output voltages and efficient energy harvesting. The whole structure has an inclination of about 45° to allow the falling droplets to hit the surface, flow on the surface, make contact with the upper electrode, and flow away, as illustrated in Fig. 1(b).

The negative charges trapped in the PTFE induce positive charges into the lower electrode, forming a charged capacitance. When the droplet hits and spreads on the PTFE surface, positive charges are also induced in the flowing droplet and an additional capacitance, C_i, is formed at the

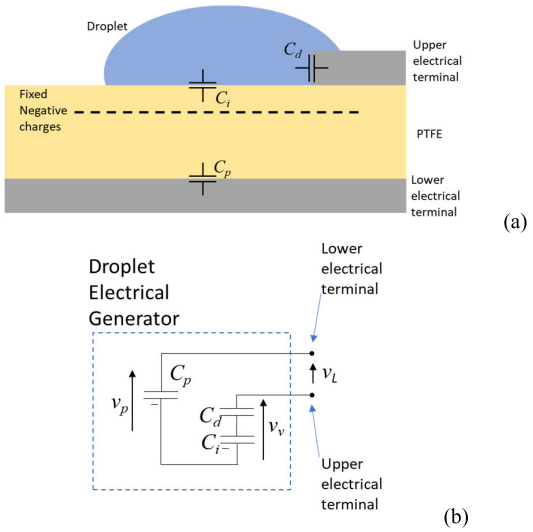

Fig. 2. (a) Structure. (b) Equivalent circuit of a DG when the droplet contacts the upper terminal.

droplet/PTFE interface. Before the droplet contacts the upper electrode, there is no charge flow through the above capacitances. By contrast, when the upper electrode and PTFE are connected by the droplet, another capacitance, C_d, is established at the droplet/upper electrode interface, as shown in Fig. 2(a), leading to the equivalent electric circuit shown in Fig. 2(b) [15], [16], [17]. Thus, if an electrical load is connected between the electrical terminals, a closed circuit is formed, which allows a current to flow through the series of the three capacitances and the external load.

The three capacitances appearing in the equivalent electrical circuit of the droplet generator can be modeled as capacitors with flat and parallel faces. In particular, with reference to the PTFE/lower-electrode capacitance, it should be highlighted that the negative trapped charges and the positive charges induced in the lower electrode are present in the entire device area. However, if $A_p(t)$ is the contact area between the droplet and the PTFE, only the charges in $A_p(t)$ contribute to the current flow when the circuit is closed. It should also be noted that when the droplet slides over the surface, $A_p(t)$ has a very limited variation, so that $A_p(t) \approx A_p$. Hence, the PTFE/lower-electrode capacitance is limited to the droplet contact area, $C_p(t)$, can be considered nearly constant and it can be expressed as

$$C_p = \frac{\varepsilon_{\text{PTFE}} A_p}{d_p} \tag{1}$$

where $\varepsilon_{\text{PTFE}}$ is the dielectric constant of the PTFE, d_p is the distance between the trapped charges and the lower electrode.

Moreover, the PTFE/droplet capacitance C_i can be expressed as

$$C_i = \frac{\varepsilon_D A_i}{\lambda_{\text{EDL}}} \tag{2}$$

where ε_D is the dielectric constant of the droplet, $A_i = A_p$ is the PTFE/droplet contact area and λ_{EDL} is the Debye width of the EDL formed in the droplet to neutralize the charged surface.

Finally, the droplet/upper-electrode capacitance C_d can be expressed as

$$C_d(t) = \frac{\varepsilon_D A_d(t)}{\lambda_{\text{EDL}}} \tag{3}$$

where $A_d(t)$ is the contact area between the droplet and the upper electrode. $A_d(t)$ is null before the contact, reaches a maximum in the time interval when the droplet flows on the upper electrode, and finally, returns to zero when the droplet goes away. The current can flow through the load only in the time interval when $A_d(t)$ is not null. The series of the two droplet capacitances C_i and $C_d(t)$ can be modeled by a single time-varying capacitance

$$C_v(t) = \frac{C_i C_d(t)}{C_i + C_d(t)}. \tag{4}$$

It is interesting to observe that, due to the time variation of $A_d(t)$, $C_v(t) = 0$ before the contact of the droplet with the upper electrode and after the end of the contact. Moreover, the time waveform of the varying capacitance $C_v(t)$ is usually characterized by a very fast increase due to the impact of the droplet on the upper electrode, followed by a slow decay due to the slow separation of the droplet from the upper terminal. Since the thickness of the PTFE is several orders of magnitude larger than the EDL width at the droplet interfaces, the maximum values taken by the capacitances formed at the droplet interfaces, C_i and C_d, are far higher than the value of the capacitance C_p, leading to $\max(C_v(t)) \gg C_p$.

The negative charge density, σ_{p0}, present in the PTFE surface makes the capacitance C_p electrically charged before any droplet reaches the PTFE surface, determining an initial voltage on the PTFE equal to

$$V_{p0} = \frac{|\sigma_{p0}| d_p}{\varepsilon_{\text{PTFE}}} = \frac{Q_{p0}}{C_p} \tag{5}$$

where Q_{p0} is the absolute value of the negative charge present in an area equal to the droplet contact area A_p. V_{p0} represents the PTFE surface voltage corresponding to the saturated value σ_{p0} of the negative charge density after a continuous droplet impingement, as deeply investigated in [15]. When the droplet contacts the upper electrode, $C_v(t)$ increases from zero and the charges Q_{p0} are reorganized between C_p and $C_v(t)$ by moving through the external load Z_L, thus inducing a current. Since the system is electrically neutral at any time, the sum of the charges on the two capacitances is constant, i.e.,

$$Q_{p0} = Q_p(t) + Q_v(t) \tag{6}$$

where $Q_p(t)$ is the charge on C_p and $Q_v(t)$ is the charge on $C_v(t)$. As shown in Fig. 2(b), it holds

$$v_L(t) = v_p(t) - v_v(t) = \frac{Q_p(t)}{C_p} - \frac{Q_v(t)}{C_v(t)} \tag{7}$$

where $v_L(t)$, $v_p(t)$ and $v_v(t)$ are the voltages on the load and on the capacitances C_p and $C_v(t)$, respectively. Hence, from (6) and (7), it results

$$v_L(t) = \frac{Q_{p0}}{C_p} - \frac{Q_v(t)}{C_t(t)} \tag{8}$$

where

$$C_t(t) = \frac{C_p C_v(t)}{C_p + C_v(t)}. \tag{9}$$

According to (8) and (5), the equivalent electric circuit in Fig. 2(b) can be reduced to the compact circuit in Fig. 3(a), made up of a constant voltage source with a value V_{p0} and a time-varying capacitance with a value $C_t(t)$. Note that the equivalent circuit in Fig. 3(a) modeling a DG is the same as that usually employed for modeling triboelectric-based electret nanogenerators, which are a particular type of electrostatic kinetic energy harvesters [24]. This model is more compact than the one shown in Fig. 2(b), [15], [16], [17], and, what is more, its parameters can be identified by measurements at the electrical terminals. In other words, as it will be shown in Section III, it avoids the direct estimation of the capacitances by using expressions (1)–(3), which would inevitably lead to very inaccurate results, also due to the unknown time waveform of the contact area $A_d(t)$.

III. Identification of Model Parameters for a Physical DG

Parameter identification is aimed at estimating, for a physical DG, the value of the initial voltage on the PTFE capacitance C_p, i.e., V_{p0}, and the time evolution of $C_t(t)$, so that the equivalent electrical model in Fig. 3(a) can be used to predict the system behavior for different electrical loads. In this section, it will be shown how to identify the circuit parameters starting from measurements at the electrical terminals of the physical DG.

In the considered case of a DG, the impedance of the measurement system cannot be neglected. The usual probe impedance of oscilloscopes is not large enough to be considered infinite and very-high impedance voltage buffers are not usually available for voltages of hundreds of volts and slew rates of several tens of volts per microsecond. For these reasons, a resistive-capacitive load, modeling the measurement system in addition to an external load, is considered at the DG electrical terminals, as shown in Fig. 3(a).

The describing equations of the equivalent circuit in Fig. 3(a) are

$$\begin{cases} \dfrac{v_L}{R_L} + C_L \dfrac{dv_L}{dt} = \dfrac{d}{dt}\left[C_t(t) v_t\right] & \text{(10a)} \\ V_{p0} = v_L + v_t & \text{(10b)} \end{cases}$$

which can be rewritten as

$$\frac{v_L}{R_L} + C_L \frac{dv_L}{dt} = V_{p0} \frac{d}{dt} C_t(t) - \frac{d}{dt}\left[C_t(t)\, v_L\right] \tag{11}$$

and, hence, in the form

$$\left[C_L + C_t(t)\right] \frac{dv_L}{dt} = -\frac{v_L}{R_L}\left[1 + R_L \frac{d}{dt} C_t(t)\right] + V_{p0} \frac{d}{dt} C_t(t). \tag{12}$$

Equation (12) is a first-order nonlinear differential equation describing the time evolution of the load voltage $v_L(t)$ as a function of time.

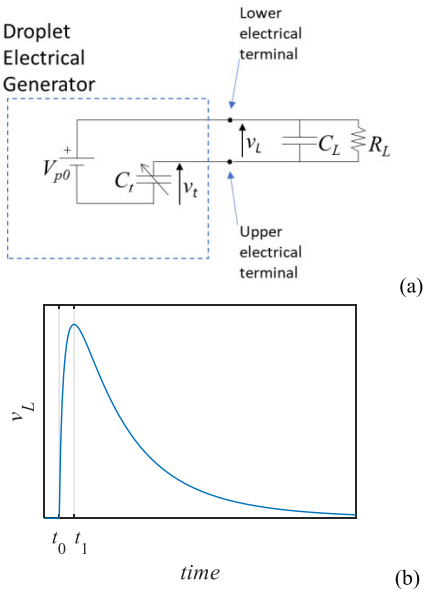

Fig. 3. (a) Compact equivalent circuit of a DG. (b) Qualitative trend of the load voltage for a resistive-capacitive load impedance.

When the load impedance is mainly capacitive, the fast initial raising of $C_v(t)$ and, hence, of $C_t(t)$, due to the frontal impact of the droplet on the upper electrode, as described in the previous section, leads to a very fast increase in the load voltage, as qualitatively shown in Fig. 3(b). Let us focus the attention on the time interval between the start of droplet-electrode contact and the voltage peak, that is (t_0, t_1). If the value of the load resistance, R_L, is high enough so that its current is negligible with respect to the current into the load capacitance, C_L, by taking into account that $v_L(t_0) = 0$ and $C_t(t_0) = 0$, the time integration of system (10) in the time interval (t_0, t_1) leads to

$$\begin{cases} C_L V_{L1} = C_{t1} V_{t1} \\ V_{p0} = V_{L1} + V_{t1} \end{cases} \tag{13}$$

where $V_{L1} = v_L(t_1)$, $V_{t1} = v_t(t_1)$ and $C_{t1} = C_t(t_1)$. From (13), (5), and (9), it results

$$Q_{p0} = \left(C_p + C_L + \frac{C_p C_L}{C_{v1}}\right) V_{L1} \tag{14}$$

where $C_{v1} = C_v(t_1)$. By considering the differences in the capacitance thicknesses mentioned in Section II, it results $C_v(t_1) = \max(C_v(t)) \gg C_p$. Therefore, (14) can be approximated as

$$Q_{p0} \cong \left(C_p + C_L\right) V_{L1}. \tag{15}$$

If the peak load voltage, V_{L1}, is measured when the system is connected to two different load capacitors, called C_{L_a} and C_{L_b}, (15) leads to the system

$$\begin{cases} Q_{p0} = \left(C_p + C_{L\_a}\right) V_{L1\_a} \\ Q_{p0} = \left(C_p + C_{L\_b}\right) V_{L1\_b}. \end{cases} \tag{16}$$

By solving system (16) with respect to the unknowns Q_{p0} and C_p, it results

$$\begin{cases} C_p = \dfrac{C_{L\_a} V_{L1\_a} - C_{L\_b} V_{L1\_b}}{V_{L1\_b} - V_{L1\_a}} \\ Q_{p0} = \left(C_p + C_{L\_b}\right) V_{L1\_b}. \end{cases} \tag{17}$$

Once the values of Q_{p0} and C_p are determined, it is possible to estimate the value of the voltage source appearing in the equivalent circuit in Fig. 3(a), i.e., $V_{p0} = Q_{p0}/C_p$.

Let us now determine the time evolution of $C_t(t)$. To this end, let us connect a very large load capacitor $C_L \gg C_p$ to the physical DG. Under this condition, it results

$$C_L \gg \frac{C_p C_v(t)}{C_p + C_v(t)} = C_t(t) \tag{18}$$

and, hence, according to (10b)

$$v_L \ll v_t \approx V_{p0}. \tag{19}$$

Thus, (10a) can be simplified as

$$\frac{v_L}{R_L} + C_L \frac{dv_L}{dt} = V_{p0} \frac{d}{dt} C_t(t). \tag{20}$$

Equation (20) is a linear differential equation in the unknown $v_L(t)$ forced by the time-varying input signal

$$q(t) = V_{p0} C_t(t). \tag{21}$$

Equation (20) shows that a DG connected to a load with very small impedance behaves like a current source of value $i_q = dq(t)/dt$, for which the feedback provided by the load and represented by the last term in (11) can be neglected.

Starting from the measured time waveform $v_L(t)$ it is possible to calculate the forcing input $q(t)$ in the Laplace domain, that is

$$Q(s) = \frac{1 + sR_L C_L}{sR_L} V_L(s) \tag{22}$$

where $V_L(s)$ is the Laplace transform of $v_L(t)$ and $Q(s)$ is the Laplace transform of $q(t)$. In other words, the output of a simple linear system with a transfer function

$$T(s) = \frac{1 + sR_L C_L}{sR_L} \tag{23}$$

forced by the measured time waveform $v_L(t)$ provides the signal $q(t)$ and the time-varying capacitance waveform

$$C_t(t) = \frac{q(t)}{V_{p0}}. \tag{24}$$

For simulation purposes, the function $C_t(t)$ can be efficiently approximated by an exponential function as

$$C_t(t) \approx k_c e^{-(t/\tau_d)^{\alpha_d}} \left[1 - e^{-(t/\tau_r)^{\alpha_r}}\right] \tag{25}$$

where τ_r and α_r affect the fast rising, whereas τ_d and α_d affect the slow decay. The parameters in (25) can be calculated by best fitting on the obtained waveform for $C_t(t)$ in (24).

Once determined V_{p0} and $C_t(t)$, all the parameters appearing in the equivalent circuit in Fig. 3(a) are identified, including the time evolution of the capacitor. By contrast, typical identification procedures assume a sinusoidal evolution of the time-varying capacitor [22], which is very far from the actual behavior of a physical DG.

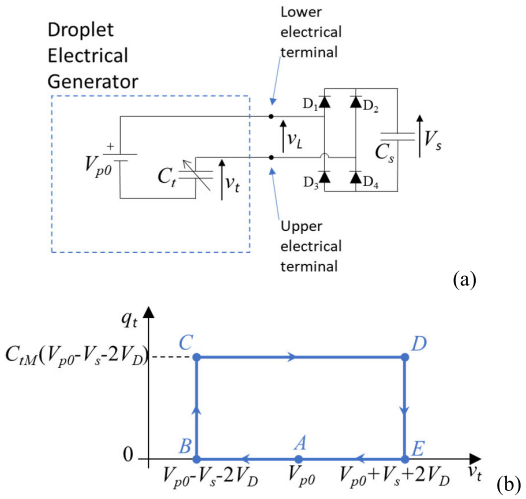

Fig. 4. (a) Schematic of a DG loaded by a diode bridge rectifier. (b) Time evolution of voltage/charge of the variable capacitance $C_t(t)$ for a single droplet.

IV. Energy Prediction

The developed model can be efficiently employed for predicting the energy extracted by the DG. The simplest electronic interface for the DG is the diode bridge in Fig. 4(a), employed for rectifying the generated ac current [16]. C_s is a very large capacitor, $C_s \gg C_t$, employed for storing the energy extracted by the DG, whose voltage, $V_s < V_{p0}$, does not vary significantly due to a single droplet. The diodes are modeled by a constant voltage, V_D, in the forward region of operation.

Before any droplet reaches the PTFE surface, $C_t(t) = 0$, the impedance of C_t is significantly higher than that of the load at the DG terminals, and, thus, $v_t = V_{p0}$. Moreover, the current i_t flowing through the variable capacitance C_t is null, and no charge is stored in it, that is $q_t = 0$, as shown by point A in Fig. 4(b).

When a droplet touches the upper electrode, the capacitance $C_t(t)$ starts to rise, the diodes are still reverse-biased, and the capacitance-voltage starts to decrease according to the law $C_t dv_t/dt = i_t - v_t dC_t/dt$, where i_t is only due to the diode leakage currents. However, the charge q_t does not increase significantly until the voltage v_t reaches a value sufficient to forward bias diodes D_1, D_4, i.e., $v_t = V_{p0} - V_s - 2V_D$, [point B in Fig. 4(b)]. Then, a significant current starts to flow through C_t, with a significant increase in its charge q_t, while the voltage stays constant. The charge rise stops when the capacitance reaches its maximum value, that is for $q_t = Q_{tM} = C_{tM}(V_{p0} - V_s - 2V_D)$, with $C_{tM} = \max(C_t)$ (point C).

Then, the capacitance starts to decrease, leading to a voltage increase that reverse biases the diodes. No current flows at the DG terminals and the charge $q_t = Q_{tM}$ stays constant until the increasing voltage $v_t(t) = Q_{tM}/C_t(t)$ reaches the value $v_t = V_{p0} + V_s + 2V_D$ (point D), which allows the current to flow through the diodes D_2, D_3. Thus, the voltage v_t is kept constant and the decrease of the capacitance reduces the charge to zero (point E). Finally, v_t tends to the initial value V_{p0} due to the high impedance of C_t and the leakage currents.

Therefore, the diode bridge rectifier implements a rectangular charge-voltage cycle for the variable capacitance C_t [25].

The energy released by C_t for a single droplet is equal to the area in the $q_t - v_t$ plane and is equal to

$$W_t = 2C_{tM}\left(V_{p0} - V_s - 2V_D\right)(V_s + 2V_D). \tag{26}$$

Since the energy lost for the leakage currents due to diodes, the storage capacitor, the capacitor load, and so on, is

$$W_L = \frac{V_s I_L}{f} \tag{27}$$

where I_L is the total leakage current and f is the frequency of the falling droplets, the energy stored in the capacitor C_s can be estimated as $W_S = W_t - W_L$, that is

$$W_S = 4W_M \cdot \times \left[\left(1 - \frac{V_s + 2V_D}{V_{p0}}\right)\frac{V_s + 2V_D}{V_{p0}} - \frac{1}{2}\frac{V_s}{V_{p0}}\frac{I_L/f}{C_{tM}V_{p0}}\right] \tag{28}$$

where $W_M = 1/2 \cdot C_{tM}V_{p0}^2$ is the maximum energy that can be converted.

Equation (28) shows that the maximum converted energy depends on the product of the initial voltage on the PTFE, V_{p0}, times the fixed negative charges $Q_{P0} = C_p V_{p0} \approx C_{tM}V_{p0}$. Moreover, the effective converted energy depends on the circuit losses and the voltage on the storage capacitor. The impact of the leakage currents and of the droplet frequency, I_L/f, on the extracted energy, still depends on the fixed negative charges $Q_{P0} = C_p V_{p0} \approx C_{tM}V_{p0}$. The optimal voltage on the storage capacitor, which ensures the maximum energy extraction, can be calculated by deriving (28) with respect to V_s and equating the result to zero, that is

$$V_{S\_\text{opt}} = \frac{V_{p0}}{2}\left(1 - \frac{I_L/f}{2C_{tM}V_{p0}}\right) - 2V_D. \tag{29}$$

Equations (28) and (29), directly deduced by the DG model, allow the designers to get a precious initial estimate for sizing the droplet generator and its electronic interface.

V. Experimental Tests

The presented approach to model a DG and to identify its parameters is here applied to a laboratory prototype of a DG made up of a PTFE sheet placed on a sheet of silver paper, acting as a lower electrode. The upper electrode is made by a simple conductive wire placed over the PTFE sheet, as shown in Fig. 5. Much more performing devices can be made by following the construction and optimization criteria shown in [15], [16], and [17], but this is out of the scope of this work. The generation of water droplets is achieved by means of a dripper connected to a tank filled with tap water.

The time waveforms of the load voltage were acquired by a 12 bit oscilloscope, Teledyne Lecroy HDO6054, in the first case when the load was made only by the oscilloscope probe, exhibiting $R_{L\_a} = 10$ MΩ and $C_{L\_a} = 10$ pF, and in a second case when a capacitor $C_E = 4598$ pF was placed in parallel to the probe, leading to an overall load characterized by $R_{L\_b} = 10$ MΩ and $C_{L\_b} = 4608$ pF. The two waveforms are reported in Fig. 6. By solving system (16) with the measured peak values of the voltage, i.e., $V_{L1\_a} = 46.55$ V and $V_{L1\_b} = 0.705$ V, the values of the initial charge $Q_{p0} = 3.2$ nC and of the PTFE capacitor $C_p = 59$ pF were calculated. From these values, the initial voltage $V_{p0} = Q_{p0}/C_p = 54.5$ V was deduced.

In order to determine the time evolution of $C_t(t)$, since $C_{L\_b} \gg C_p$, the load voltage waveform measured for

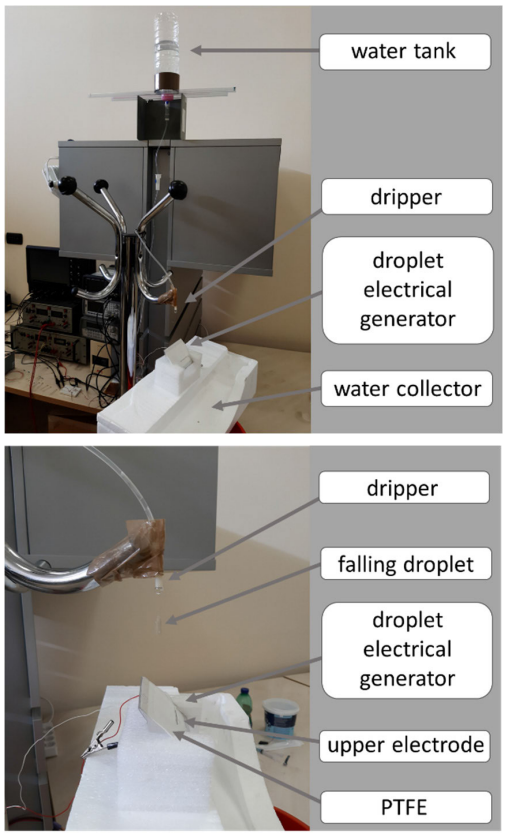

Fig. 5. (a) Photograph of the experimental setup and (b) is a zoom of (a).

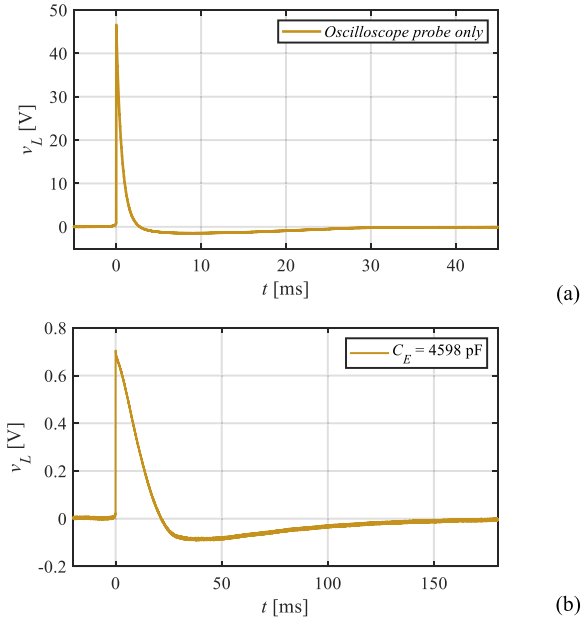

Fig. 6. Measured voltages at the terminals of the DG (a) when it is loaded by the oscilloscope probe only and (b) when it is loaded by an additional capacitor equal to $C_E = 4598$ pF.

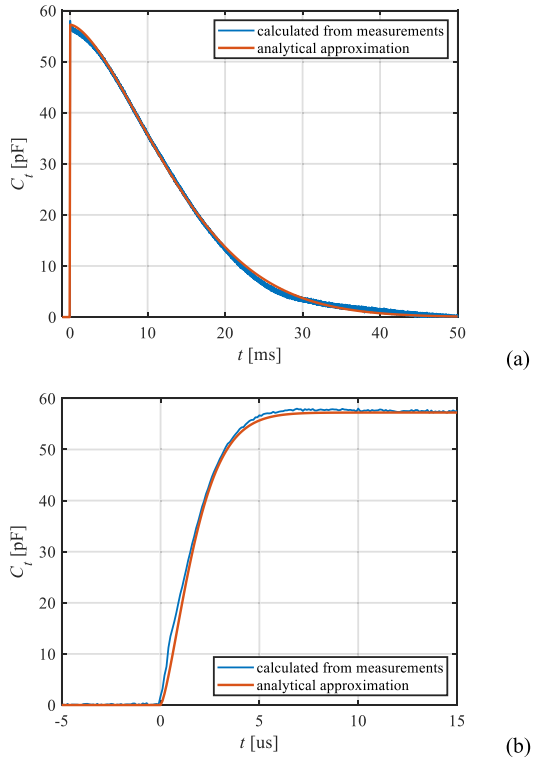

Fig. 7. Time evolution of $C_t(t)$, as calculated from laboratory measurements and its analytical approximation. (a) Complete time waveform and (b) zoom of the initial rising.

$R_{L\_b} = 10$ MΩ and $C_{L\_b} = 4608$ pF, was exploited as input to the linear system with the transfer function reported in (23). The calculated output of the linear system, $q(t)$, allowed us to calculate $C_t(t)$, as shown in Fig. 7. The calculated time waveform was approximated by best fitting with the function in (25) with the coefficients $k_c = 0.97C_p$, $\tau_d = 16$ ms, $\alpha_d = 1.6$, $\tau_r = 2$ μs, $\alpha_r = 1.4$. The approximated function is also reported in Fig. 7.

The equivalent model with the identified parameters was validated through the comparison of the measured waveforms with the results from SPICE simulations of the proposed model in Fig. 3(a). Since most circuit simulators do not allow to simulate time-varying capacitors, this component was implemented through the equivalent circuit in Fig. 8. Indeed, a two-terminal made up of a capacitor having a constant value C_0 in series with a voltage-controlled voltage source of value $v_x = [1 - f(t)]v_t$, with $f(t)$ an arbitrary time function, draws a current equal to

$$i_t = C_0 \frac{d}{dt}\left[v_t - v_x\right] = \frac{d}{dt}\left[C_0 f\left(t\right) v_t\right]. \tag{30}$$

Thus, the considered two terminals behave like a time-varying capacitor of value $C_T(t) = C_0 f(t)$.

A first comparison of measurements and simulations was performed by connecting different capacitors C_E to the electrical terminals of the droplet generator. These capacitors lie in parallel with the oscilloscope probe impedance characterized by $R_m = 10$ MΩ and $C_m = 10$ pF, resulting in a load impedance having $R_L = R_m$ and $C_L = C_m + C_E$. The measured waveforms and the simulated waveforms are reported in Fig. 9. It is interesting to observe that the simulated circuit

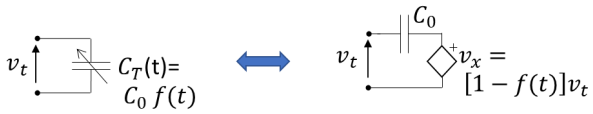

Fig. 8. Emulation of a time-varying capacitor through a series of a constant capacitor and a voltage source.

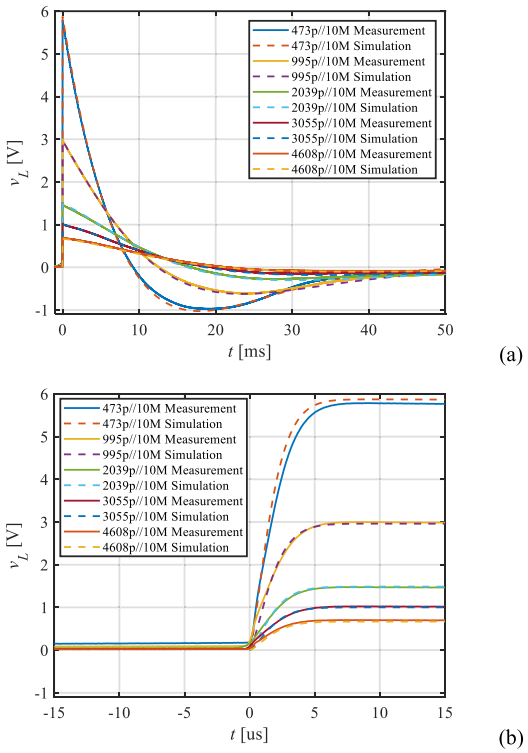

Fig. 9. Measured and simulated waveforms for different values of the load impedance with $R_L = 10$ MΩ. (a) Full waveforms. (b) Zoom of the initial transients.

well fits the measured waveforms both in the case of the load waveform used for identifying the circuit parameters, i.e., the curve for $C_L = 4608$ pF, and in the case of different values of the load capacitance.

A second set of measurement-simulation comparisons was performed by connecting an additional resistor R_E at the electrical terminals of the droplet generator, so that $R_L = R_m // R_E$ and $C_L = C_m + C_E$. The comparison reported in Fig. 10(a) and in Fig. 10(b) using different time scales, shows that the proposed model is able to predict with good accuracy the system behavior in very different load conditions, not only when the value of R_L is large as assumed during the identification procedure, but also for smaller values.

In order to highlight the ability of the model to predict the harvested energy, the comparison between the energy per drop experimentally measured and that predicted by the developed model is shown in Fig. 11 for a load made up of a resistor $R_L = R_m$ with a parallel capacitor $C_L = C_m + C_E$. The prediction error, also reported in the same Figure, shows the good accuracy of the model for practical purposes.

Finally, the identified model of the droplet generator was simulated in the configuration of Fig. 4(a), i.e., connected to a diode bridge rectifier. For the diodes, the low leakage types 1N3595 by Onsemi were considered, whose accurate SPICE models are provided by the manufacturer. The storage capacitor was set to $C_s = 1\mu$F. The time evolution of

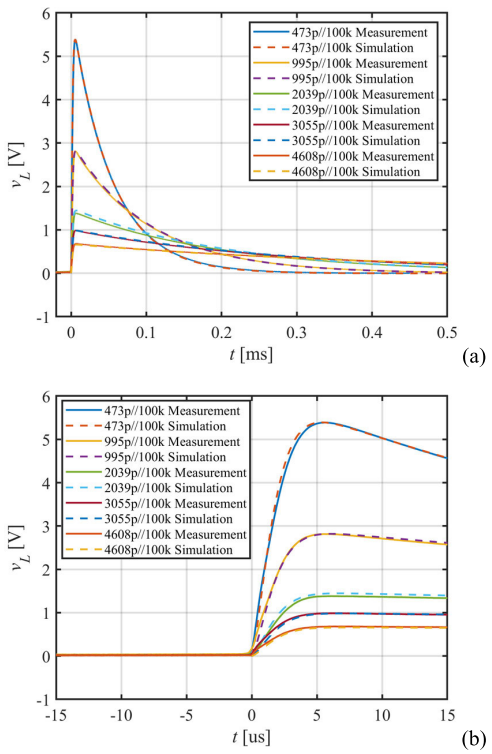

Fig. 10. Measured and simulated waveforms for different values of the load impedance with $R_L = 100$ kΩ. (a) Full waveforms. (b) Zoom of the initial transients.

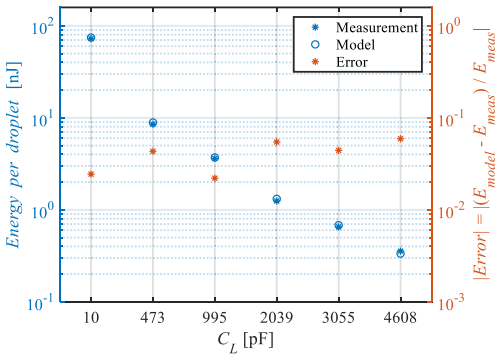

Fig. 11. Comparison of the energy per droplet measured and predicted by model. Absolute values on the left axis and error on the right axis.

the voltage and charge of the variable capacitance $C_t(t)$ obtained by simulations are reported in Fig. 12(a) for different values of the initial voltage V_s. The same figure also reports the analytical approximations for the same quantities. The comparison shows that the approximated equations reported in Section IV provide a good estimation of the $q_t - v_t$ cycle, whose area gives the energy extracted by the droplet generator. In particular, (28), relating the converted energy to the droplet generator parameters and to the rectifier characteristics, can be usefully exploited for design, as shown in Fig. 12(b). There, the converted energy normalized to its maximum value is shown as a function of the storage capacitor voltage and of the ratio between the leakage current and the droplet frequency. It can be observed that, according to (29), the optimal value of V_s decreases for increasing values of losses and for decreasing values of frequency. Moreover, the converted energy significantly decreases with the leakage currents. As an example, for

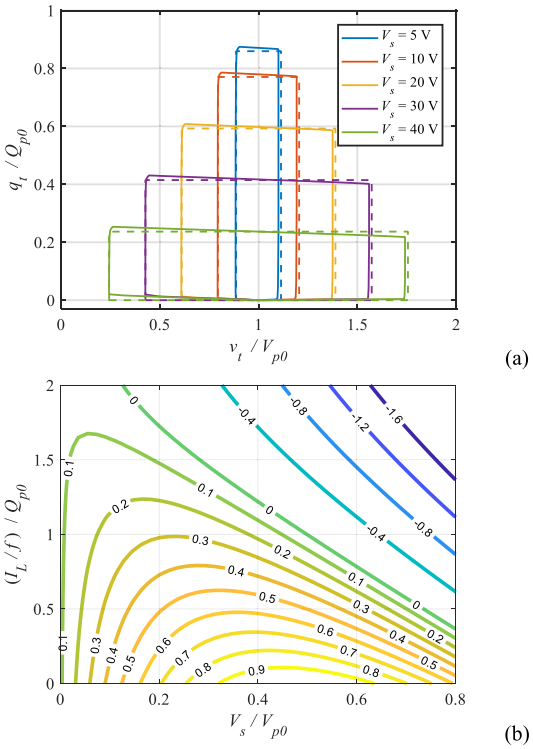

Fig. 12. (a) Time evolution of the voltage and charge of the variable capacitance $C_t(t)$ for a single droplet, as obtained by SPICE simulations (continuous lines) and as predicted by theoretical analysis (dashed lines). (b) Normalized energy stored in the storage capacitor, W_S/W_M, as a function of the normalized capacitor voltage, V_s/V_{p0}, and of the normalized leakage losses, $(I_L/f)/Q_{p0}$.

$I_L/f = Q_{p0}$ the converted energy does not exceed one-third of the theoretical maximum value expected for zero losses.

VI. Conclusion

A compact equivalent circuit of a DG has been presented and the procedure for determining its parameters from electrical measurements on a physical prototype has been outlined. The obtained model is simple enough to allow the analytical prediction of the extracted energy as a function of the generator characteristics and the load properties. Therefore, the presented results can be exploited by designers for analyzing and building optimized energy harvesters.

In future works, the behavior of the DG will be investigated, when connected to more sophisticated electrical interfaces in order to increase the extracted energy.

References

[1] Y.-W. Chong, W. Ismail, K. Ko, and C.-Y. Lee, "Energy harvesting for wearable devices: A review," *IEEE Sensors J.*, vol. 19, no. 20, pp. 9047–9062, Oct. 2019, doi: 10.1109/JSEN.2019.2925638.

[2] W. Liao, Z. Zhang, X. Huang, L. Zhang, S. Wang, and J. Kan, "A novel magnetic-coupling non-contact piezoelectric wind energy harvester with a compound-embedded structure," *IEEE Sensors J.*, vol. 22, no. 9, pp. 8428–8438, May 2022, doi: 10.1109/JSEN.2022.3161833.

[3] Z. L. Wang, T. Jiang, and L. Xu, "Toward the blue energy dream by triboelectric nanogenerator networks," *Nano Energy*, vol. 39, pp. 9–23, Sep. 2017, doi: 10.1016/j.nanoen.2017.06.035.

[4] R. Guigon, J.-J. Chaillout, T. Jager, and G. Despesse, "Harvesting raindrop energy: Experimental study," *Smart Mater. Struct.*, vol. 17, no. 1, Feb. 2008, Art. no. 015039, doi: 10.1088/0964-1726/17/01/015039.

[5] T. Alkhaddeim, B. Al Shujaa, W. Al Beiey, F. Al Neyadi, and M. Al Ahmad, "Piezoelectric energy droplet harvesting and modeling," in *Proc. IEEE SENSORS*, Oct. 2012, pp. 1–4, doi: 10.1109/ICSENS.2012.6411440.
[6] Y. Wang, S. Gao, W. Xu, and Z. Wang, "Nanogenerators with superwetting surfaces for harvesting water/liquid energy," *Adv. Funct. Mater.*, vol. 30, no. 26, Jun. 2020, Art. no. 1908252, doi: 10.1002/adfm.201908252.
[7] W. Xu and Z. Wang, "Fusion of slippery interfaces and transistor-inspired architecture for water kinetic energy harvesting," *Joule*, vol. 4, no. 12, pp. 2527–2531, Dec. 2020, doi: 10.1016/j.joule.2020.09.007.
[8] P. R. Adhikari, N. T. Tasneem, R. C. Reid, and I. Mahbub, "Electrode and electrolyte configurations for low frequency motion energy harvesting based on reverse electrowetting," *Sci. Rep.*, vol. 11, no. 1, Mar. 2021, Art. no. 5030, doi: 10.1038/s41598-021-84414-3.
[9] P. R. Adhikari, M. N. Islam, Y. Jiang, R. C. Reid, and I. Mahbub, "Reverse electrowetting-on-dielectric energy harvesting using 3-D printed flexible electrodes for self-powered wearable sensors," *IEEE Sensors Lett.*, vol. 6, no. 5, pp. 1–4, May 2022, doi: 10.1109/LSENS.2022.3170207.
[10] Z. Yang, E. Halvorsen, and T. Dong, "Power generation from conductive droplet sliding on electret film," *Appl. Phys. Lett.*, vol. 100, no. 21, pp. 213905-1–213905-4, 2012.
[11] Z. Yang, E. Halvorsen, and T. Dong, "Electrostatic energy harvester employing conductive droplet and thin-film electret," *J. Microelectromech. Syst.*, vol. 23, no. 2, pp. 315–323, Apr. 2014, doi: 10.1109/JMEMS.2013.2273933.
[12] Z.-H. Lin, G. Cheng, S. Lee, K. C. Pradel, and Z. L. Wang, "Harvesting water drop energy by a sequential contact-electrification and electrostatic-induction process," *Adv. Mater.*, vol. 26, no. 27, pp. 4690–4696, Jul. 2014, doi: 10.1002/adma.201400373.
[13] W. Xu et al., "SLIPS-TENG: Robust triboelectric nanogenerator with optical and charge transparency using a slippery interface," *Nat. Sci. Rev.*, vol. 6, no. 3, pp. 540–550, May 2019, doi: 10.1093/nsr/nwz025.
[14] S.-B. Jeon, D. Kim, G.-W. Yoon, J.-B. Yoon, and Y.-K. Choi, "Self-cleaning hybrid energy harvester to generate power from raindrop and sunlight," *Nano Energy*, vol. 12, pp. 636–645, Mar. 2015, doi: 10.1016/j.nanoen.2015.01.039.
[15] W. Xu et al., "A droplet-based electricity generator with high instantaneous power density," *Nature*, vol. 578, no. 7795, pp. 392–396, Feb. 2020, doi: 10.1038/s41586-020-1985-6.
[16] Z. Li et al., "A droplet-based electricity generator for large-scale raindrop energy harvesting," *Nano Energy*, vol. 100, Sep. 2022, Art. no. 107443, doi: 10.1016/j.nanoen.2022.107443.
[17] N. Zhang et al., "A droplet-based electricity generator with ultrahigh instantaneous output and short charging time," *Droplet*, vol. 1, no. 1, pp. 56–64, Jul. 2022, doi: 10.1002/dro2.10.
[18] L. Costanzo, A. L. Schiavo, M. Vitelli, and L. Zuo, "Optimization of AC–DC converters for regenerative train suspensions," *IEEE Trans. Ind. Appl.*, vol. 58, no. 2, pp. 2389–2399, Mar. 2022, doi: 10.1109/TIA.2021.3136145.
[19] L. Costanzo, M. Liu, A. L. Schiavo, M. Vitelli, and L. Zuo, "Backpack energy harvesting system with maximum power point tracking capability," *IEEE Trans. Ind. Electron.*, vol. 69, no. 1, pp. 506–516, Jan. 2022, doi: 10.1109/TIE.2021.3053896.
[20] L. Costanzo, A. Lo Schiavo, and M. Vitelli, "Improving the electromagnetic vibration energy harvester performance by using a double coil structure," *Appl. Sci.*, vol. 12, no. 3, 2022, Art. no. 1166, doi: 10.3390/app12031166.
[21] C. Wang and A. Riaud, "Mathematic and numerical analysis of droplet-based electricity generator," in *Proc. IEEE 15th Int. Conf. Solid-State Integr. Circuit Technol. (ICSICT)*, Nov. 2020, pp. 1–3, doi: 10.1109/ICSICT49897.2020.9278178.
[22] R. Hinchet, A. Ghaffarinejad, Y. Lu, J. Y. Hasani, S.-W. Kim, and P. Basset, "Understanding and modeling of triboelectric-electret nanogenerator," *Nano Energy*, vol. 47, pp. 401–409, May 2018, doi: 10.1016/j.nanoen.2018.02.030.
[23] R. Panigrahi and S. K. Mishra, "An electrical model of a dielectric elastomer generator," *IEEE Trans. Power Electron.*, vol. 33, no. 4, pp. 2792–2797, Apr. 2018, doi: 10.1109/TPEL.2017.2749329.
[24] S. Boisseau, G. Despesse, and B. A. Seddik, "Electrostatic conversion for vibration energy harvesting," in *Small-Scale Energy Harvesting*. Rijeka, Croatia: InTech, 2012, pp. 91–134, doi: 10.5772/51360.
[25] D. Galayko et al., "Capacitive energy conversion with circuits implementing a rectangular charge-voltage cycle—Part 1: Analysis of the electrical domain," *IEEE Trans. Circuits Syst. I, Reg. Papers*, vol. 62, no. 11, pp. 2652–2663, Nov. 2015, doi: 10.1109/TCSI.2015.2451911.

Luigi Costanzo was born in Italy, in 1989. He received the master's degree (cum laude) in electronic engineering from the Second University of Naples, Naples, Italy, in 2014, and the Ph.D. degree in industrial and information engineering from the Department of Industrial and Information Engineering, Università degli Studi della Campania "Luigi Vanvitelli," Aversa, Caserta, Italy, in 2017.

He is currently an Assistant Professor with the Department of Engineering of Università degli Studi della Campania "Luigi Vanvitelli." His main research interests include maximum power point tracking techniques in photovoltaic applications, power electronics circuits for renewable energy sources, analysis, and design and optimization of energy harvesting systems.

Alessandro Lo Schiavo (Senior Member, IEEE) was born in Naples, Italy, in 1972. He received the Laurea degree (cum laude) in electronic engineering from the Università degli Studi di Napoli, Naples, Italy, in 1997, and the Ph.D. degree in electrical energy conversion from the Seconda Università degli Studi di Napoli, Aversa, Caserta, Italy, in 2000.

From 2001 to 2017, he was an Assistant Professor at the Dipartimento di Ingegneria dell'Informazione, Seconda Università degli Studi di Napoli, Caserta, Italy. In 2017, he was appointed as an Associate Professor of electronics at the Università degli Studi della Campania "Luigi Vanvitelli," Aversa, where he teaches fundamentals of microelectronics and the design of electronic circuits. His current research interests include electronic circuits for energy harvesting, wireless sensor networks, analysis and design of analog circuits, and nonlinear circuit theory.

Prof. Lo Schiavo is an Associate Editor of *International Journal of Circuit Theory and Applications Applied Sciences,* and *Mathematical Problems in Engineering*.

Massimo Vitelli was born in Caserta, Italy, in 1967. He received the laurea degree (cum laude) in electrical engineering from the University of Naples Federico II, Naples, Italy, in 1992.

He is currently a Full Professor with the Department of Engineering, Università degli Studi della Campania "Luigi Vanvitelli," Aversa, Caserta, Italy, where he teaches electric circuits and power electronics. He has been engaged in many scientific national projects. He has coauthored a number of national and international patents and two scientific books. His main research interests include maximum power point tracking techniques in photovoltaic applications, power electronics circuits for renewable energy sources, methods for analysis, and the design and optimization of energy harvesting systems.

Prof. Vitelli is an Associate Editor of the IEEE TRANSACTIONS on POWER ELECTRONICS.

Open Access funding provided by 'Università degli Studi della Campania "Luigi Vanvitelli"' within the CRUI CARE Agreement